Modeling Radiation Forces Acting on Topex/Poseidon for Precision Orbit Determination

J. Andrew Marshall*
NASA Goddard Space Flight Center, Greenbelt, Maryland 20771
Scott B. Luthcke†
Hughes STX, Lanham, Maryland 20706

Geodetic satellites, such as GEOSAT, SPOT, ERS-1, and TOPEX/Poseidon require accurate orbital computations to support the scientific data they collect. The TOPEX/Poseidon mission requirements dictate that the mismodeling of the nonconservative forces of solar radiation, Earth albedo and infrared reradiation, and spacecraft thermal imbalances produce in combination no more than a 6-cm radial rms orbit error over a 10-day period. Therefore, a box-wing satellite form has been investigated to model the satellite as the combination of flat plates arranged in the shape of a box and a connected solar array. The nonconservative forces acting on each of the eight surfaces are computed and adjusted independently, yielding vector accelerations which are summed to compute the total aggregate effect on the satellite center of mass. Acceleration profiles from finite element analysis are compared to those from the boxwing model, and these tests indicate that modeling solar radiation pressure acceleration is relatively straightforward. However, the thermal imbalance modeling is made much more complicated given the satellite's complex attitude control law and its relation to the predicted temperature history for each surface.

Nomenclature

A = surface area of the flat plate, m^2
a = cold equilibrium surface temperature, K
c = speed of light, m/s
c_T = delta temperature between cold and hot equilibrium, K
d = transition time from hot to cold equilibrium temperature, s
f = transition time from cold to hot equilibrium temperature, s
G = radiation flux from source
M = satellite mass, kg
N = total number of plates
n = surface normal vector
s = source incidence vector
s_1 = shift parameter to ensure continuity
s_2 = shift parameter to ensure continuity
T = temperature, K
t_1 = time since shadow exit, s
t_2 = time since shadow entry, s
x = rotation rate/thermal inertia constant
β' = angle between Earth-sun vector and orbit plane
Γ = acceleration due to radiation pressure on the flat plate, m/s^2
γ = solar array pitch angle
δ = diffusive reflectivity, percentage of total incoming radiation
ϵ = emissivity
θ = angle between surface normal and solar incidence
θ_{shd} = angle between normal and sun vectors at shadow entry
θ_{sun} = angle between normal and sun vectors at shadow exit
ρ = specular reflectivity, percentage of total incoming radiation
σ = Stefan-Boltzmann constant, 5.67E-08 W/m^2/K^4
ψ = yaw angle
Ω = orbit angle

Subscripts
i = plate of interest
j = Earth spot of interest

Introduction

THE Ocean TOPography EXperiment (TOPEX/Poseidon or T/P) spacecraft was launched on an Ariane rocket on August 10, 1992. This is a joint mission between NASA and the French Centre National d'Etudes Spatiales (CNES) to study the Earth's ocean circulation. It is a dedicated altimetry mission using one dual frequency (US) and one solid-state (French) radar altimeter to precisely measure the ocean topography. The spacecraft is in a circular "frozen" orbit at an altitude of 1336 km and an inclination of 66 deg, resulting in a groundtrack that repeats every 10 days.

When combined with a precision orbit ephemeris, the altimetric measurements yield observations of the sea surface height. To fully exploit the capabilites of the altimeters and to satisfy the accuracy requirements of the oceanographic community, the orbit error must not exceed 13-cm radial rms over a 10-day orbit repeat period.[1] Orbit determination of this accuracy has never before been undertaken or achieved for a satellite at T/P's altitude.

The common method for computing the radiation pressure upon orbiting satellites within the orbit determination software has been to ignore these rotating, attitude controlled, geometrically complex shapes and to treat the satellite form as a symmetrically perfect and rotationally invariant sphere, or so-called cannonball. A typical cannonball radiation pressure model has a constant projected area with respect to the radiation source, and empirical scaling factors are commonly adjusted to improve the orbital fit to the tracking data. In addition, the thermal emission of the spacecraft itself is ignored. These approaches are not adequate to meet the required 6-cm radial rms error budget for modeling the radiation forces on T/P over a 10-day period. Others have made detailed assessments of some of the nonconservative forces acting on specific satellites.[2-7] However, their models are not directly applicable to T/P. After considerable analysis of all surface force contributions, resultant models to be used in T/P orbit determination have been derived and are presented herein.

*Aerospace Engineer, Space Geodesy Branch. Member AIAA.
†Senior Scientific Programmer/Analyst, 4400 Forbes Blvd.

TOPEX/Poseidon Spacecraft

The TOPEX/Poseidon spacecraft has an intricate attitude control system due to its large, single axis gimbal solar array. Perfect solar pointing (sun incidence vector normal to the solar array) requires the spacecraft to yaw about its Earth-pointing Z axis at rates which exceed the capabilities of the attitude control system. Therefore, the spacecraft builder designed a sinusoidal yaw command which achieves near perfect solar pointing while remaining within attitude control system limits.[8] The algorithm is based on the coordinate systems shown in Figs. 1b and 2. The spacecraft body-fixed system origin is within the vehicle body, although not at the center of mass, with the positive Y axis pointing opposite to the solar array axis, the positive Z axis directed to the Earth nadir, and the positive X axis orthogonal to the Y and Z axes to complete the right-handed system. The inertial system is centered at the geocenter with the X_0 axis normal to the satellite orbit plane, the Z_0 axis points in the direction of the sun as projected into the orbit plane, and the Y_0 axis normal to these axes. As shown in Fig. 2, β' refers to the angle between the sun vector and the orbit plane, and Ω is the orbit angle, measured from the Y_0 axis. The actual yaw angle ψ of the spacecraft is rotated positively from the X_p axis (the along track direction) about
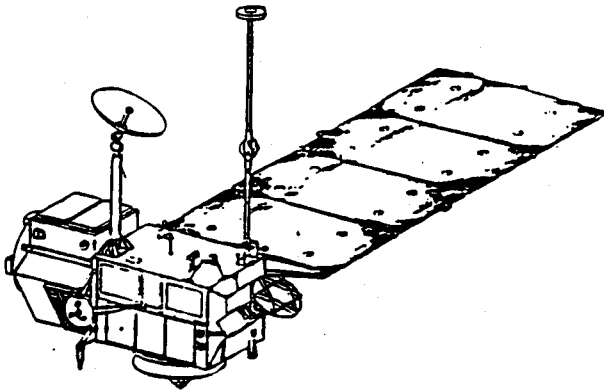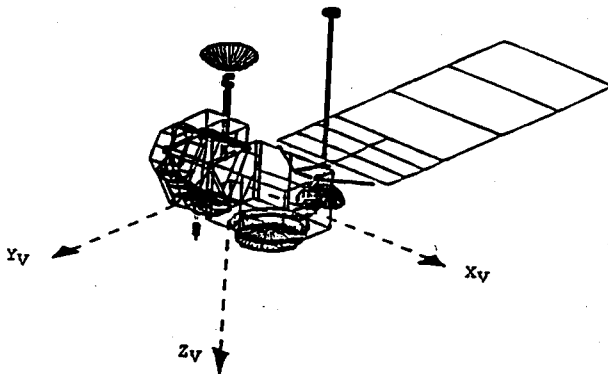

Fig. 1a   TOPEX/Poseidon spacecraft.
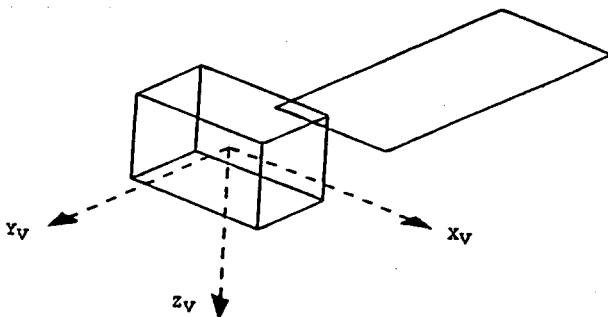

Fig. 1b   Micromodel approximation.

Fig. 1c   Macromodel approximation.

the Z axis and is determined from the β' and Ω. The solar array pitch angle γ rotates positively from the spacecraft X axis about the Y axis to orient the cells toward the sun for optimum sun pointing.

Model Development

The first step in a detailed analysis of the radiation forces acting on T/P was to accurately compute the radiation forces due to the sun, Earth albedo, Earth infrared, and spacecraft thermal emissions upon T/P with the use of a finite element model of the spacecraft. This investigation generated acceleration histories at a wide variety of β' and orbit angles, referred to as the micromodels. A thorough explanation of this modeling effort is given by Antreasian and Rosborough.[9] Since a precise thermal and radiative model of a spacecraft is necessarily computationally intensive, this micromodel, which served as a "truth" model, was computed offline. A relatively simple and less computationally intensive model, or macromodel, more suitable for precision orbit computations, was devised and tested to emulate the micromodel accelerations. This model was introduced by Marshall et al.[10] A graphical representation of this development is shown in Fig. 1.

This concept is based on approximating the satellite shape with a combination of flat plates. The nonconservative forces acting on each of the composite surfaces are computed independently. All plate interaction effects, such as shadowing, reflection, and conduction are ignored. This yields vector accelerations which are summed to compute the total effect on the spacecraft center of mass. The algorithm includes the ability to adjust aggregate parameters associated with each flat plate. The macromodel can then be fit or "tuned" to the actual satellite acceleration history based on orbit errors sensed from laser tracking data and from telemetered satellite on-orbit temperatures. For T/P, a box-wing shape was chosen with the plates aligned along the satellite body-fixed coordinate system (Fig. 1).

Solar and Earth Radiation

Solar, Earth albedo, and Earth infrared emissions are the three external radiative fluxes acting on a spacecraft. The radiation pressure acting on a flat plate can be computed using the following equation,[11] assuming a Lambertian diffusion:

$$\Gamma = -\frac{GA \cos \theta}{Mc} \left[2(\delta/3 + \rho \cos \theta)n + (1 - \rho)s \right]$$

The adjustable parameters are area and specular and diffusive reflectivity. These parameters are averaged values which represent the consolidation of the spacecraft's complex shapes and material properties into a single, homogeneous flat plate.

The albedo and infrared contributions use a similar acceleration equation to the solar radiation. However, the flux mag-
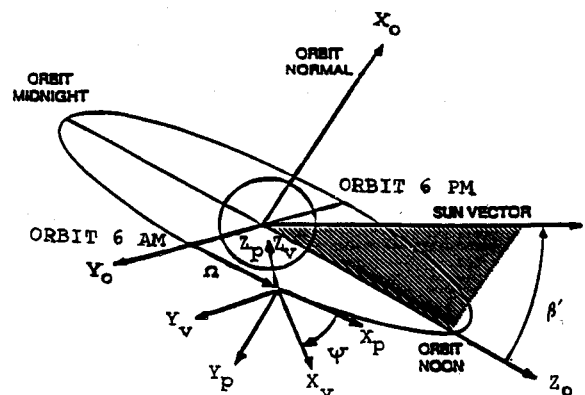

Fig. 2   TOPEX/Poseidon inertial coordinate system.[8]

nitude is different. Also, the source vector is the Earth grid spot-to-satellite vector rather than the solar incidence vector. The spot definition and location are defined by Knocke et al.[12] The total albedo/infrared acceleration can be expressed as

$$\Gamma = -\sum_i^N \sum_j^{19} \frac{G_j A_i \cos \theta_{ij}}{Mc} [2(\delta_i/3 + \rho_i \cos \theta_{ij})n_i + (1 - \rho_i)s_j]$$

Spacecraft Radiation

Two separate types of fluxes affect the flat plate temperatures: internal and external. Internally, the equipment dissipates radiation which serves to heat the satellite surfaces. Externally, the solar radiation, albedo, and infrared fluxes cause surface heating. The force exerted on a surface due to thermal emission, assuming a Lambertian diffusion function, can be expressed as

$$F = -\frac{2A\sigma}{3c} \epsilon T^4 n$$

The temperature history algorithm, however, is not as clearly defined. One must take into account the complexities of 1) occultation effects, 2) oblique illumination, and 3) the spacecraft's thermal inertia, without losing sight of the need for simplicity and generality.

The temperature for a surface exposed to sunlight is modeled as

$$T = a + c_T * \cos(\theta/x)[1 - \exp(-t_1/f)]$$

and while in shadow as

$$T = a + c_T \exp(-t_2 + s_2/d)$$

$$s_2 = -d \ln \{\cos(\theta_{shd}/x)[1 - \exp(-t_1/f)]\}$$

The adjustable parameters are area, emissivity, and all five temperature terms (a, c_T, d, f, x).

An explanation of these equations is appropriate. First, note that solar radiation is the only direct effect influencing the temperature. That is to say, the θ angle and the time parameters are based only on solar illumination and neglect the albedo and IR effects. However, albedo and IR indirectly influence the a priori values of all of the adjustable temperature parameters. A plate's orientation with respect to the sun dictates which temperature algorithm to use. The cosine term in the sunlight equation allows for the fact that an obliquely illuminated plate will have a lower temperature than one perpendicular to the sun vector. In contrast, a plate's cooling pattern, when occulted by either the Earth or the spacecraft, is independent of the sun position; therefore, no such allowance needs to be made. The x parameter in the denominator of the cosine term accounts for the fact that the temperature is not directly proportional to the rate at which spacecraft rotation moves a plate from direct to oblique illumination. Without x, there is no delay in reaching the cold equilibrium value as the plate enters shadow. The exponential term addresses the occultation transition effects. As a face enters or leaves shadow, its temperature can be approximated by an exponential curve. A different time constant (d or f) is applied depending on whether the surface is heating or cooling. Finally, a shift term is introduced to ensure continuity in the transition from the sunlight to shadow temperature equation. This assumes that the plate will reach its cold equilibrium temperature in shadow before heating begins. Given that this assumption is not true, a different set of shift parameters must be established. For example, during sinusoidal yaw the $X-$ face of T/P is occulted only by the Earth. As β' increases, this shadow time gradually decreases. Therefore, the plate will always reach its hot equilibrium temperature and not necessarily reach its cold equilibrium temperature. In this case the following temperature history algorithms are used.

Sunlight:
$$T = a + c_T * \cos(\theta/x)\{1 - \exp[-(t_1 + s_1)/f_i]\}$$

where
$$s_1 = -f \ln [1 - \exp(-t_2/d)(\cos \theta_{shd}/\cos \theta_{sun})]$$

Shadow:
$$T = a + c_T * \cos \exp[-(t_2 + s_2)/d]$$

where
$$s_2 = -d \ln \cos(\cos \theta_{shd}/x)$$

More simplistic representations have been implemented with varying success. However, they all fail to replicate certain thermal behaviors exhibited by the micromodel. A model of this complexity is necessary to meet T/P mission requirements; therefore, this is the chosen parameterization for T/P modeling.

Results

To test the validity of these macromodels, a comparison has been performed between the acceleration histories predicted at a wide variety of β' and orbit angles by the macro- and micromodels. A Bayesian least squares estimation procedure has been used to tailor the adjustable macromodel parameters to better fit the micromodel generated acceleration histories for the solar radiation and the thermal imbalance nonconservative forces as outlined by Marshall et al.[13] A priori values with realistic uncertainties served to constrain some certain highly correlated parameters and, as a result, cannot be recovered independently. Specifically, the solar array parameters were not adjusted since their properties are relatively well known, and they do not represent an average of many smaller surfaces of varying characteristics. Also, to ensure realistic temperature values, the equilibrium temperatures a and c were constrained so as not to stray more than a few degrees from

Table 1 Orbital parameters

Semi-major axis, km	a	7714
Eccentricity	e	0.00
Inclination, deg	i	66
Argument of perigee, deg	ω	90
Altitude, km	h	1336.00
Nodal precession rate, deg/day	Ω	-2.31
Period, min	P	112

Table 2 Macromodel plate normal vectors in the spacecraft body-fixed system

Plate	X	Y	Z
$X+$	1.0	0.0	0.0
$X-$	-1.0	0.0	0.0
$Y+$	0.0	1.0	0.0
$Y-$	0.0	-1.0	0.0
$Z+$	0.0	0.0	1.0
$Z-$	0.0	0.0	-1.0
$SA+$	1.0	0.0	0.0
$SA-$	-1.0	0.0	0.0

Table 3 Plate optical and thermal characteristics for tuned solar radiation pressure model

	$X+$	$X-$	$Y+$	$Y-$	$Z+$	$Z-$	$SA+$	$SA-$
Area	3.74	3.77	8.27	8.07	8.67	8.44	21.4	21.44
Specular ref.	0.201	0.244	0.886	0.782	0.239	0.275	0.05	0.17
Diffuse ref.	0.375	0.386	0.302	0.339	0.390	0.363	0.22	0.66
Emissivity	0.769	0.995	0.873	0.714	0.770	0.746	0.87	0.88
Temp. A	181	168	191	190	240	103	236	234
Temp. C	233	178	18	63	98.5	125	110	96
Time D	621	282	759	426	519	680	805	806
Time F	111	120	624	487	767	413	828	866
Theta$X$	1.25	1.00	1.05	1.00	1.06	1.15	1.00	1.00

the values predicted by the micromodel. Parameters associated with the $X+$, $Y+$, $Y-$, and solar array (SA)$-$ faces exhibited the weakest recovery due to their limited solar exposure. To date, the solar radiation and thermal imbalance forces have been fit independently, and appropriate parameters have been recovered. Therefore, nonphysical properties could result when the terms are considered jointly. With the delivery of the "as-built" spacecraft models, new micromodels will be generated, and a more aggressive and thorough macromodel parameter recovery will be undertaken. These adjusted values will be adopted as nominal values in the actual precision orbit determination computations.

All of the macromodels described herein have been implemented in the precision orbit determination software package at NASA/Goddard Space Flight Center (GSFC), GEODYN.[14] The results presented in this paper use GEODYN and the T/P macromodels to simulate a 10-day T/P orbit. Table 2 describes the individual plate normal vectors in the satellite body-fixed system used in the box-wing representation of the T/P spacecraft. Table 3 shows the actual macromodel parameter values used in this testing as derived from the least squares adjustment outlined previously. It is important to note that a constant value of 0.34 for Earth albedo and 0.68 for Earth

emissivity were used to represent the Earth albedo and IR forces. These values were used as constants to be consistent with the micromodel generation. Marshall et al.[13] gives a comprehensive discussion of results for all of the radiative forces acting on T/P. In the interest of brevity, only the solar radiation acceleration results will be discussed in detail herein whereas the other force model results will only be quantified.

Solar Radiation

Solar radiation is the dominant radiative force acting on T/P. Its acceleration profile is driven by the large area of the solar array which tracks the sun throughout the orbit. Plots of the micromodel solar radiation acceleration in the along track, cross track, and radial directions are shown in Figs. 3, 4, and 5. Data spacing is at 4-deg β' increments and 15-deg orbit angle increments. The U-shaped outline of the Earth occultation region is clearly visible. At $\beta' = 0$ deg the spacecraft is in fixed yaw and the sun is edge on to the orbit plane. Therefore, the plots correctly display no cross track acceleration, a sinusoidal signal in the radial direction, and a similar signal offset 90 deg in phase in the along track component. T/P is in a sinusoidal yaw at $\beta' = 40$ deg and the almost constant cross
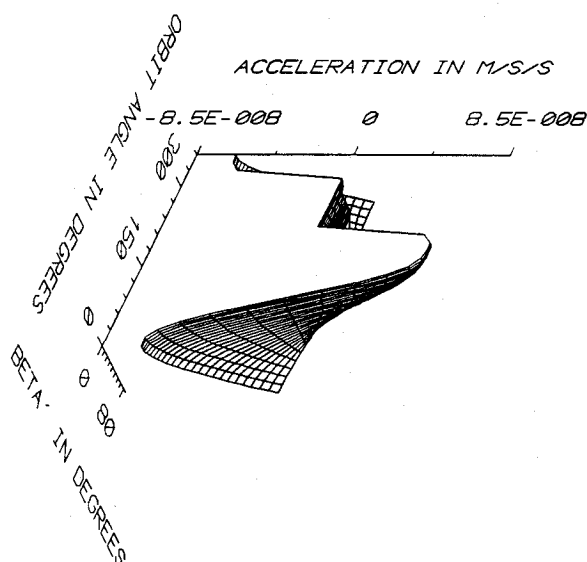

Fig. 3   Micromodel solar radiation pressure along track acceleration.
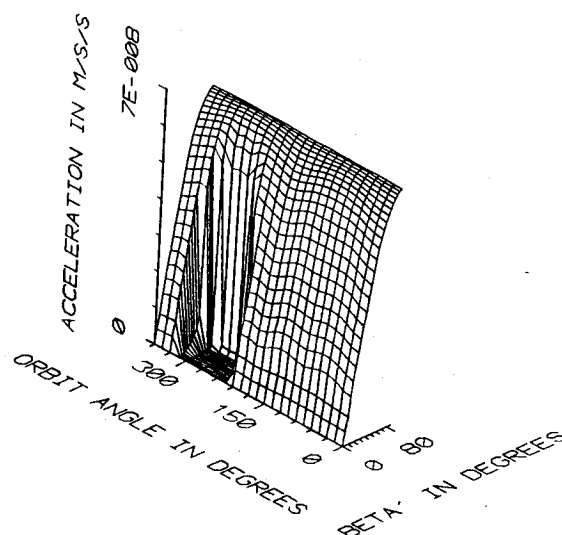

Fig. 5   Micromodel solar radiation pressure radial acceleration.
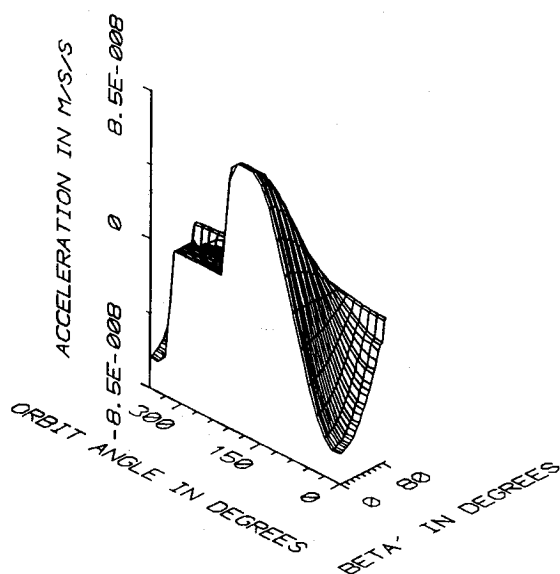

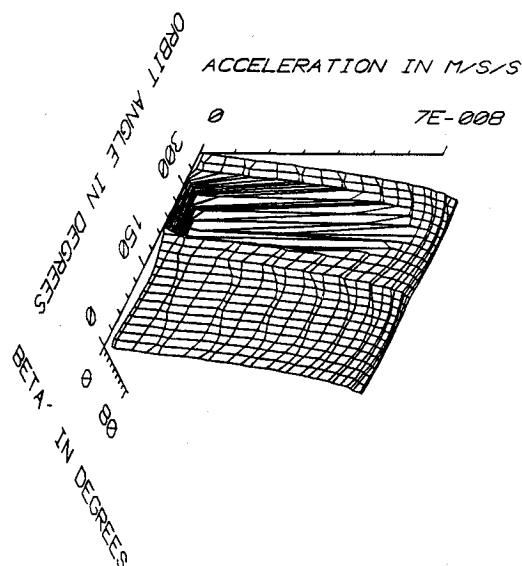Fig. 4   Micromodel solar radiation pressure cross track acceleration.

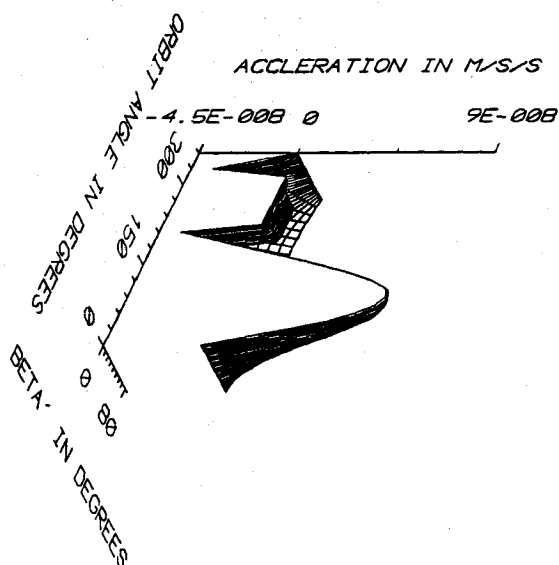Fig. 6   Macromodel solar radiation pressure along track acceleration.

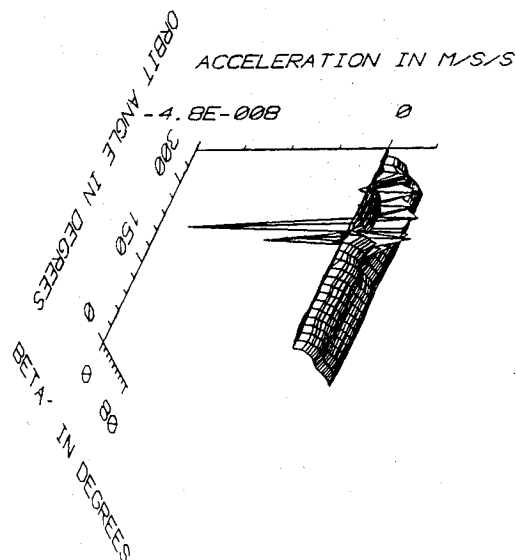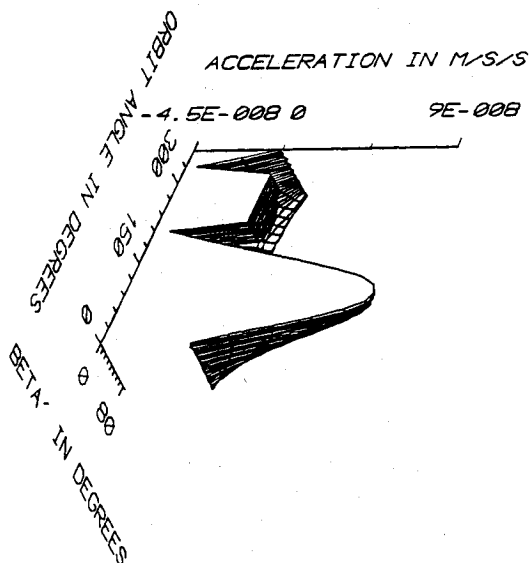Fig. 7 Macromodel solar radiation pressure cross track acceleration.

Fig. 8 Macromodel solar radiation pressure radial acceleration.

Fig. 9 Along track solar radiation pressure acceleration residuals: (macro − micro) mean = − 3.8E-11; rms = 4.3E-9.

Fig. 10 Cross track solar radiation pressure acceleration residuals: (macro − micro) mean = 1.7E-9; rms = 4.3E-9.

Fig. 11 Radial solar radiation pressure acceleration residuals: (macro − micro) mean = 1.3E-9; rms = 4.9E-9.
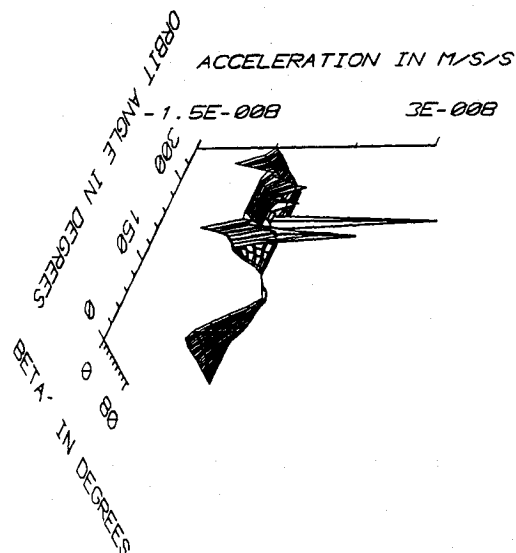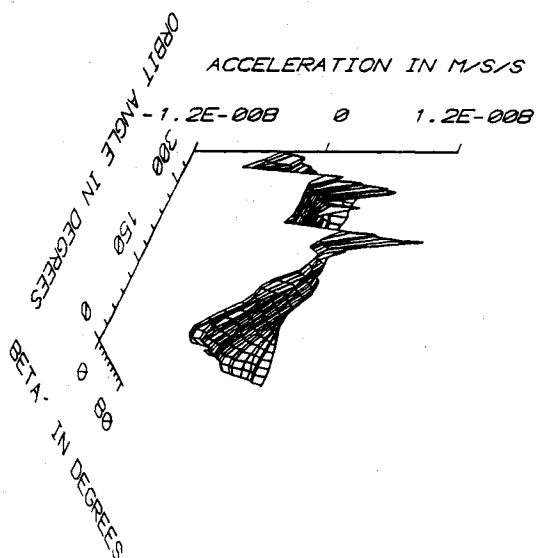
track force drops to zero during occultation. The along track and radial accelerations have smaller amplitudes but virtually the same shape as $\beta' = 0$ deg. At $\beta' = 88$ deg, the spacecraft is in continuous sunlight, the sun is nearly perpendicular to the orbit plane, and the cross track acceleration dominates.

As exhibited in Figs. 6, 7, and 8, the macromodel was exercised in GEODYN to generate data for comparison with the micromodel. Notice that the macromodel captures all of the features of the micromodel, even though the profiles change drastically throughout the different β' regimes. The residuals between the micro- and macromodels in each of the three directions are displayed in Figs. 9–11. The prominent residual spikes appearing around the Earth occultation boundary are caused by a different definition of this boundary's location in the micro- and macromodels and, therefore, is not a problem since GEODYN calculates shadow entry and exit times using a precise conical model. It is anticipated that the remaining residual exhibited in the along track and radial residual plots will be greatly reduced with proper tuning of the solar array macromodel parameters.

Table 4   Modelability and error analysis summary

Force	Rms of micromodel force for β' of 0–88 deg and orbit angle of 0–360 deg	Rms of macro-micromodel residuals	Rms radial 10-day orbit error (for all components)
Solar along track	3.2×10^{-8} M/S^2	4.3×10^{-9} M/S^2	
Solar cross track	4.5×10^{-8} M/S^2	4.3×10^{-9} M/S^2	
Solar radial	2.7×10^{-8} M/S^2	4.9×10^{-9} M/S^2	
Total radial orbit error for 10-day arc			5.1 cm
Albedo along track	6.1×10^{-10} M/S^2	2.3×10^{-10} M/S^2	
Albedo cross track	8.3×10^{-10} M/S^2	3.3×10^{-10} M/S^2	
Albedo radial	4.6×10^{-9} M/S^2	2.4×10^{-10} M/S^2	
Total radial orbit error for 10-day arc			2.1 cm
IR along track	6.1×10^{-10} M/S^2	5.4×10^{-10} M/S^2	
IR cross track	7.4×10^{-10} M/S^2	5.3×10^{-10} M/S^2	
IR radial	5.6×10^{-9} M/S^2	5.4×10^{-10} M/S^2	
Total radial orbit error for 10-day arc			2.2 cm
Thermal along track	2.0×10^{-9} M/S^2	1.0×10^{-9} M/S^2	
Thermal cross track	3.6×10^{-10} M/S^2	5.9×10^{-9} M/S^2	
Thermal radial	1.5×10^{-10} M/S^2	5.6×10^{-9} M/S^2	
Total radial orbit error for 10-day arc			5.2 cm

Modelability and Error Analysis

The results presented in the previous sections have given a measure of the macromodel success in modeling satellite accelerations. Mission requirements, however, dictate that model performance be evaluated in terms of radial orbit error. To quantify the radial orbit error produced by macromodel errors, the following analysis was performed.

The micromodel acceleration histories are considered by default to be truth. Certainly, they are the result of a very rigorous analysis and are the best representation of truth that is currently available. Thus, any mismodeling by the macromodel is represented by the macro − micro model acceleration residual histories previously discussed. During this analysis, each of the macromodel force errors were considered individually. This was necessary, since each force was individually tuned to the micromodel. The exceptions are the Earth albedo and IR, which simply use the solar model tuned parameter values.

GEODYN was modified to include a routine that does a bilinear interpolation (over β' and Ω) on the micromodel acceleration data for each of the forces considered (solar, albedo, IR, and thermal). Thus, micromodel accelerations were computed at integration step time within the GEODYN software. The micromodel GEODYN version produced four data sets containing true-of-date X, Y, Z orbit data for a 10-day T/P arc, using each of the micromodel accelerations in turn. A 30-s integration step size was used for all of the runs, and the data generation interval was 180 s. The particular 10-day arc spans a β' region of 10.5–36 deg. Therefore, this arc covers the fixed yaw to sinusoidal yaw regime, and the analysis is weighted toward the acceleration residuals in this region. Four separate data reduction runs using the macromodel accelerations were made on the four micromodel generated data sets. Thus, for each individual force considered, the only difference in the force modeling between the data generation and data reduction runs is the particular macro − micro model difference. Only the state, a single drag coefficient, and a single solar radiation pressure coefficient were adjusted over the 10-day arc interval. The adjustment of specific macromodel parameters was not part of this study and is addressed extensively in a companion report.[15] The radial rms orbit error was computed from the residuals of the macromodel-fit orbit to the micromodel-generated orbit.

Table 4 gives the modelability and error analysis summary. The rms radial orbit errors over a 10-day T/P arc for each of the individual macromodel forces is less than 6 cm, demonstrating that each individual macromodel meets mission re-

quirements. It should be stressed that these results were achieved without adjusting T/P macromodel specific parameters and that the inclusion of these parameters does improve modelability and reduce the orbit errors.[15] The modelability of the along track and cross track albedo and IR accelerations is poor. However, the surface properties used to describe the albedo and IR models were never tuned to the micromodels, and currently the solar model parameter set is employed. The modelability of the accelerations do improve when macromodel parameters are adjusted.[15] Furthermore, the radial component of the albedo and IR accelerations is an order of magnitude larger than the other components. The modelability of this component is quite good. The along track thermal acceleration also demonstrates deficiencies due to problems in modeling and tuning the X − plate temperature. Further model tuning is necessary for this X − face. The solar radiation pressure is currently modeled at the 10% level and is anticipated to improve with the tuning of the solar array diffuse and specular reflectivity parameters. The analysis shows that with no adjustment of the macromodel surface-specific parameters and a minimal adjusted parameter set, the individual macromodel errors meet mission requirements. However, the error produced by the sum of the nonconservative forces must meet the 6-cm radial rms mission requirement. This analysis could not be properly performed since a combined force parameter set had not yet been developed but is addressed in a companion paper.[15] To get an estimate of the combined force error, the analysis was performed using the combined micro- and macromodel forces. The thermal model tuned parameter set was used in this analysis. Adjusting the state, a single drag coefficient, and a single solar radiation pressure coefficient, the radial rms orbit error of a 10-day arc was 6.98 cm. A short run was made including the adjustment of the solar array front diffuse reflectivity parameter and demonstrated marked improvement, giving a hint of the type of improvement expected when macromodel parameters are adjusted.

Conclusions

To meet precision orbit determination requirements for geodetic satellite missions, specifically, TOPEX/Poseidon, detailed models of the radiative forces acting on the spacecraft have been constructed. Solar, Earth albedo, Earth infrared, and the spacecraft's thermal radiation effects have all been considered. A detailed finite element analysis has been performed to compute the total force and induced accelerations

acting on the satellite. This required a precise description of the satellite shape, material properties, and attitude control algorithm. Because these models are too computationally intensive to be incorporated into the orbit determination software, a more simplistic model which approximates the finite element acceleration profiles has been developed. It is based on depicting the satellite as a combination of flat plates and computing the nonconservative forces acting on each plate independently. These acceleration vectors are summed to produce the overall effect on the satellite center of mass. For T/P, a box-wing shape is used. Each plate has associated parameters which can be adjusted to improve model performance with respect to the micromodel analysis and, when the spacecraft is on orbit, to the tracking observations. The adequacy of these macromodels has been assessed through direct comparison with the micromodels. The effect of these residuals on the orbit error budget has been studied. Analyses indicate these precise models individually meet mission requirements. It has been shown that improved modelability will be achieved when macromodel specific parameters are adjusted.

Acknowledgments

References

[1]Stewart, R., Fu, L. L., Lefebvre, M., "Science Opportunities from the TOPEX/Poseidon Mission," Jet Propulsion Lab., Pub. 86-18, July 1986.

[2]Fliegel, H. F., Gallini, T. E., and Swift, E. R., "Global Positioning System Radiation Force Model for Geodetic Applications," *Journal of Geophysical Research*, Vol. 97, No. B1, 1992, pp. 559–568.

[3]Scharroo, R., Wakker, K. F., Ambrosius, B. A. C., and Noomen, R., "On the Along-Track Acceleration of the LAGEOS Satellite," *Journal of Geophysical Research*, Vol. 96, No. B1, 1991, pp. 729–740.

[4]Rubincam, D. P., and Weiss, N. R., "The Orbit of LAGEOS and Solar Eclipses," *Journal of Geophysical Research*, Vol. 90, No. B11, 1985, pp. 9399–9402.

[5]Rubincam, D. P., and Weiss, N. R., "Earth Albedo and the Orbit of LAGEOS," *Celestial Mechanics*, Vol. 38, No. 3, 1986, pp. 233–296.

[6]Rubincam, D. P., "LAGEOS Orbit Decay Due to Infrared Radiation from Earth," *Journal of Geophysical Research*, Vol. 92, No. B2, 1987, pp. 1287–1294.

[7]Rubincam, D. P., "Yarkovsky Thermal Drag on LAGEOS," *Journal of Geophysical Research*, Vol. 93, No. B11, 1988, pp. 13805–13810.

[8]Perrygo, C., "TOPEX Satellite Yaw Maneuvers," Fairchild Space Co., Fairchild IOC Ref.: 968:SE:87-074, Germantown, MD, Nov. 1987.

[9]Antreasian, P. G., and Rosborough, G. W., "Prediction of Radiant Energy Forces on the TOPEX/POSEIDON Spacecraft," *Journal of Spacecraft and Rockets*, Vol. 29, No. 1, 1992, pp. 81–90.

[10]Marshall, J. A, Luthcke, S. B., Antreasian, P. G., and Rosborough, G. W., "Modeling Radiation Forces Acting on Satellites for Precision Orbit Determination," *Proceedings of the AAS/AIAA Astrodynamics Conference*, (Durango, CO), AAS Paper 91-357, Aug. 1991.

[11]Milani, A., Nobili, A. M., and Farinella, P., "Non-Gravitational Perturbations and Satellite Geodesy," Adam Hilger, Bristol, England, UK, 1987, p. 49.

[12]Knocke, P. C., Ries, J. C., and Tapley, B. D., "Earth Radiation Pressure Effects on Satellites," *Proceedings of the AIAA/AAS Astrodynamics Conference*, (Washington, DC), AIAA Paper 88-4292, Aug. 1988, pp. 577–586.

[13]Marshall, J. A, Luthcke, S. B., Antreasian, P. G., and Rosborough, G. W., "Modeling Radiation Forces Acting on TOPEX/Poseidon for Precision Orbit Determination," NASA TM 104564, May 1992.

[14]Putney, B. H., Rowton, S., Williams, D. A., McCarthy, J. J., Pavlis, D., Luthcke, S. B., and Tsaoussi, L., "GEODYN II System Description," STX Systems Corp., Lanham, MD, 1991.

[15]Luthcke, S. B., and Marshall, J. A., "Nonconservative Force Model Parameter Estimation Strategy for TOPEX/Poseidon Precision Orbit Determination," NASA TM 104575, Nov. 1992.